Development of delivery system based on marine chitosan: Encapsulationand release kinetic study of antioxidant peptides from chitosan microparticle

Rim Nasri, Marwa Hamdi, Sana Touir, S.M. Li, Maha Karra-Chaâbouni, Moncef Nasri

Development of delivery system based on marine chitosan: Encapsulation and release kinetic study of antioxidant peptides from chitosan microparticle

Rim Nasri [a,b,*], Marwa Hamdi [a], Sana Touir [a], Suming Li [c], Maha Karra-Chaâbouni [a], Moncef Nasri [a]

[a] Laboratory of Enzyme Engineering and Microbiology, University of Sfax, National Engineering School of Sfax, B.P. 1173-3038, Sfax, Tunisia
[b] Higher Institute of Biotechnology of Monastir, University of Monastir, 5000, Taher Haddad Street, Monastir, Tunisia
[c] Institut Européen des Membranes, IEM-UMR 5635, Univ Montpellier, ENSCM, CNRS, 34095 Montpellier, France

ARTICLE INFO

Article history:
Received 24 June 2020
Received in revised form 12 November 2020
Accepted 13 November 2020
Available online xxxx

Keywords:
Chitosan microparticles
Biopeptides
Antioxidant activity
Encapsulation
Delivery system
Kinetic release

ABSTRACT

The present work aims to encapsulate goby fish protein hydrolysate (GPH), endowed with antioxidant activity, through ionic gelation process using blue crab chitosan (CH) and tripolyphosphate anions and to evaluate the structural, thermal and antioxidant properties of the elaborated microparticles (MPs). The GPH-loaded MPs present spherical shape as seen by scanning electron microscopy (SEM) images and positive zeta potential. The increase of loaded GPH concentration led to the increase of encapsulation efficiency (EE) and to the reduction of the particle size. In fact, MPs, loaded with 2 and 5 mg/ml GPH, had EE values of 44 and 58% and mean particles size of 4.81 and 3.78 μm, respectively. Furthermore, thermogravimetric analysis (TGA) profiles revealed the enhanced thermal stability of encapsulated biopeptides compared to the free ones. Release kinetic data showed a Fickian diffusion behavior which follows swelling and a diffusion-controlled mechanism for peptides liberation. Finally, as opposed to unloaded MPs, an improvement of the antioxidant activity of the loaded MPs with biopeptides was observed.

1. Introduction

There is a great interest in the marine fish peptides, as dietary supplements, based on their functional and biological activities that have an impact on human health [1]. Indeed, derived fish bioactive peptides, especially, those prepared by an enzymatic procedure, have led to an enormous attention to nutraceutical and pharmaceutical industries, owing to their broad spectrum of bioactivities, such as antihypertensive [2], anti-inflammatory [3], anticoagulant [4], antioxidant [5,6], antidiabetic [7] activities. In our previous study, goby protein hydrolysate (GPH) prepared using triggerfish proteases were found to display an interesting anti-ACE and antioxidant activities. Furthermore, its incorporation in turkey meat sausage efficiently reduced lipid peroxidation [5]. Interestingly, oral administration of GPH to Wistar rats, fed a hypercaloric diet, contributed to the prevention of renal toxicity and restores the antioxidant parameters in both liver and kidney [8]. Taking into consideration these finding, GPH could be used as a natural antioxidant dietary supplement in preventing oxidation reactions in food processing. For instance, oral administration and delivery of bioactive peptides were well studied and the potentiality of peptides, including antioxidant peptides, were proved *in silico* and *in vivo* works, which make them a potential supplementary dietary product. However, there are several technical limitations to overcome before the successfully delivered of bioactive proteins, such as their probable gastrointestinal hydrolysis and their bitter taste [9].

Microencapsulation is an innovative method that permits bioactive molecules to be entrapped within a polymer matrix. It is an effective process to control the release of peptides and to avoid their degradation. Several biopolymers had been described to be used as a wall matrix to encapsulate peptides, such as lipids [10] and carbohydrates [11,12]. Numerous reports described the efficiency of peptides encapsulation through chitosan matrix [13,14]. Chitosan has been potentially used for the development of particles owing to their biodegradability, non-toxicity and biocompatibility. Characterized by its positive charge, chitosan could form particles in acid conditions using the ionotropic gelation technique with tripolyphosphate (TPP). The obtained systems are closely investigated for their controlled release of bioactive molecules and might, consequently, be employed as a promising carrier agent of bioactive molecules [12].

Therefore, the present study focused primarily on the conception of chitosan microparticles in order to encapsulate GPH peptides. The physicochemical and structural characteristics of the elaborated microparticles were investigated. Similarly, the encapsulation efficiency (EE), *in vitro* release mechanism, and antioxidant activity of unloaded and loaded CH-based MPs were determined.

* Corresponding author at: Laboratory of Enzyme Engineering and Microbiology, University of Sfax, National Engineering School of Sfax, B.P. 1173-3038, Sfax, Tunisia.
E-mail address: rymnasri2@gmail.com (R. Nasri).

2. Materials and methods

2.1. Materials

Sodium tripolyphosphate (TPP) was purchased from Sigma-Aldrich. DPPH (2, 2-diphenyl-1-picrylhydrazyl), ferrozine, $FeCl_2$, ethylenediaminetetraacetic acid (EDTA), butylated hydroxyanisole (BHA), NaOH powder were procured from Sigma Chemical Co. (St. Louis, MO, USA).

2.2. Elaboration of goby protein hydrolysate

GPH was prepared as described in our previous work [4]. First of all, goby proteins were digested using triggerfish digestive proteases at 50 °C and pH 10.0, with enzyme/protein ratio of 1:3 (U/mg). During the reaction, the pH was adjusted to the desired value by the addition of NaOH solution (4 N). Then, the enzymatic reaction was stopped by the heat treatment of the sample at 80 °C for 10 min. Finally, GPH was recovered after centrifugation at 10,000*g* for 20 min and then freeze-dried (Moduloyd-230, Thermo-Fisher Scientific, USA).

2.3. Extraction of chitosan from blue crab shell

Chitosan (CH) was obtained from blue crab *Portunus segnis* shells following the method of Hamdi et al. [15]. First, chitin was extracted through enzymatic deproteinization of dried blue crab shell using Purafect®, and then by the chemical demineralization step (three successive HCl (0.55 M) baths at 4 °C during 30 min for each bath). Afterwards, the extracted chitin was converted to CH by the alkaline treatment with 12.5 M NaOH at a ratio of 1:10 (w/v) for 4 h at 140 °C. The average molecular weight of the obtained CH was estimated to be 125 kDa and with an acetylation degree of 11%.

2.4. Preparation of GPH-loaded chitosan microparticles

GPH-loaded CH microcapsules were elaborated by the ionic gelation technique as described by Hosseini et al. [6]. Briefly, CH solution (50 ml) was prepared at a concentration of 1% in 0.15 M (v/v) acetic acid at pH 4.0 for 24 h. GPH was then added to the CH solution at different concentrations (2 and 5 mg/ml). Afterwards, the TPP solution was added dropwise into the CH solution under a magnetic stirring at 300 rpm to reach a CH/TPP weight ratio of 1/0.22. Subsequently, the resultant microparticles (MPs) were recuperated after centrifugation at 3000*g* for 30 min and at 4 °C. The MPs were rinsed with ultrapure water, freeze-dried, and stored at −20 °C. The MPs, enriched with GPH concentration of 2 and 5 mg/ml, are named, respectively, GPH2- and GPH5-loaded MPs. The unloaded chitosan microparticles (unloaded MPs), used as a blank, were prepared following the same methodology without the addition of GPH.

2.5. Characterization of GPH-loaded MPs

2.5.1. Particle size and zeta-potential measurements

Measurements of mean particles size, size distribution and zeta potentials of the CH-based MPs were determined by a laser scattering particles size distribution Litesizer 500 (Anton Paar, GmbH, France) based on dynamic light scattering. Each sample (10 mg/ml) was analyzed in triplicate and the mean value was reported.

2.5.2. Fourier transform infrared measurement

Fourier transform infrared (FTIR) analyses of the CH, GPH and MPs were performed in transmission mode using a FTIR spectroscopy (NEXUS of ThermoFisher, Germany) containing a diamond/ZnSe crystal. Measurements were achieved at ambient temperature and were recorded in the range of 4000–700 cm^{-1}. Data analysis and treatment were carried out through the OMNIC Spectra software (ThermoFisher Scientific).

2.5.3. Scanning electron microscope analysis

The morphological characterization of GPH-loaded MPs was recorded using a scanning electron microscopy (SEM, Hitachi S-4800) under an accelerating voltage of 2.0 kV and an absolute pressure of 60 Pa, after sputter coating with a 5 nm thick gold.

2.5.4. Thermogravimetric analysis (TGA)

Thermal stability analyses of GPH, CH and MPs were recorded using Thermogravimetric analyzer (TGA, Q500 High Resolution, TA Instruments), operating under nitrogen flow (60 ml/min). TGA analysis is based on the assessment of the progressive change in mass, expressed in percentage (%), as function of temperature. Samples were heated from 25 to 700 °C at a heating rate of 20 °C/min and their weight, which, initially, was around 4 mg, was constantly measured with an accuracy of 0.01 mg. Thermograms were analyzed using the TA Universal V4.5A software.

2.6. Determination of encapsulation efficiency (EE) and loading capacity (LC)

EE, which described the amount of peptides entrapped into the MPs, was estimated by subtracting the free biopeptides present in the supernatant from the initial GPH concentration used for the chitosan-based MPs preparation. The unloaded peptides, present in the supernatant, were estimated by the Lowry method [16]. The LC is the amount of peptides loaded per unit weight of the nanoparticle.

The EE and LC were calculated by the following equations,

$$EE\ (\%) = ((W_T - W_F)/W_T) \times 100$$

$$LC\ (\%) = ((W_T - W_F)/W_{MPs}) \times 100$$

where W_T and W_F represent the weights of the total and the unloaded GPH peptides, respectively. W_{MPs} represents the weight of recovered MPs after freeze-drying.

2.7. In vitro biopeptides release study

Biopeptides, released from MPs, were determined as follows: GPH-loaded MPs (20 mg) were dispersed in 10 ml of phosphate buffer saline (PBS, pH 7.4) and incubated at room temperature. At different time intervals (1–16 h), 1 ml of the release medium was taken out, and an equal volume of fresh buffer was added. The amount of released peptides at each time point was determined by the colorimetric method of Lowry et al. [16]. The absorbance was converted into percentage release using a standard calibration curve and experiments were performed in triplicates in order to ensure accuracy. The release profiles of biopeptides from chitosan MPs were analyzed by applying the zero order (cumulative percent drug release *vs* time), first order (log cumulative percent drug release *vs* time), Higuchi's kinetics (cumulative percent drug release *vs* √time), and Korsmeyer-Peppas equation (log cumulative percentage of drug release *vs* log time):

$$\text{Zero order model}: Q_t/Q_\infty = Kt;$$

$$\text{First order model}: Q_t/Q_\infty = 1 - e^{-Kt};$$

$$\text{Higuchi model}: Q_t/Q_\infty = Kt^{1/2t};$$

$$\text{Korsmeyer-Peppas model}: Q_t/Q_\infty = Kt^n.$$

where $\mathbf{Q_t}$ represents the percentage of biopeptides released at time t, and $\mathbf{Q_\infty}$ represents the total percentage of biopeptide released; $\mathbf{Q_t/Q_\infty}$

is the fractional release of drug at time t. **k** is the release rate constant and **n** is the diffusional exponent which could indicate the biopeptides release mechanism and **t** is the time.

2.8. Determination of antioxidant activities

The DPPH free radical-scavenging activity of MPs was determined as described by Bersuder, Hole & Smith [17], with slight modifications. Briefly, 10 mg of MPs sample were added to 500 μl distilled water, 375 μl of 99.5% ethanol and 125 μl of 0.02% DPPH that was dissolved in 95% ethanol. The mixture was homogenized, vigorously and then kept for 4 h in the dark; the absorbance was recorded at 517 nm. Lower absorbance of the reaction mixture indicated higher DPPH free radical-scavenging activity. DPPH radical-scavenging activity was calculated as follows:

$$\textit{Scavenging activity}\ (\%) = \frac{\text{A control} + \text{A blank} - \text{A sample}}{\text{A control}}$$

where $A_{control}$ is the absorbance of the reaction containing all reagents except the MPs, A_{blank} is the absorbance of the reaction containing all reagents except the DPPH and A_{sample} is the absorbance of the reaction mixture. The experiment was carried out in triplicate and the results are mean values.

The chelating activity of samples towards ferrous ion (Fe^{2+}) was determined according to the method of Decker & Welch [18], with slight modifications. 10 mg of MPs was mixed with 4.7 ml of distilled water. The mixture was then reacted with 0.1 ml of 2 mM $FeCl_2$, $4H_2O$ and 0.2 ml of 5 mM 3-(2-pyridyl)-5,6-bis(4-phenyl-sulfonic acid)-1,2,4-triazine (ferrozine) for 20 min at room temperature. The absorbance was then read at 562 nm. The control was conducted in the same manner except that distilled water was used instead of the sample. The blank was conducted in the same manner except the ferrozine. The chelating activity (%) was calculated as follows:

$$\text{Ferrous chelating activity}\ (\%) = \frac{\text{A contol} + \text{A blank} - \text{A sample}}{\text{A control}} \times 100$$

2.9. Statistical analysis

All experiments were carried out at least in three replicates and mean values with standard deviation errors (SD), were stated. Mean separation and significance were analyzed using the SPSS software package ver. 17.0 professional edition (SPSS, Inc., Chicago, IL, USA) using the ANOVA analysis. Differences were considered significant at $p < 0.05$.

3. Results and discussion

3.1. Characterization of microparticles

3.1.1. Zeta potential and particle size of MPs

In the CH-based MPs were elaborated using the ionic-crosslinking 204 gelation process among an amino group of glucosamine ring of CH and the negative charged 205 groups of TPP [19,20]. The zeta potential analysis is gaining information about the surface charge and the dispersion stability of MPs. So, particles with zeta potential values above +30 mV or below −30 mV are considered as a stable system, owing to mutual electrostatic repulsion and overcoming the aggregation of particles [21]. Overall, all microparticles presented zeta potential values that were higher than 30 mV, indicating that CH-based MPs could be considered as stable system (Table 1). The occurrence of positive surface charge could be due to the contribution of cationic groups (NH_3^+) of both chitosan and biopeptides. Furthermore, results, reported in Table 1, reveal that loading 2 mg/ml of GPH into CH solution significantly decreased the zeta potential value of MPs ($p < 0.05$) [12]. Thus, the reduction of the MPs surface charge with the addition of biopeptides could be explained by the involvement of the amino groups in electrostatic interactions. However, the zeta potential of MPs increased once again, when the biopeptides contents of MPs were increased from 2 to 5 mg/ml, indicating that GPH5-loaded MPs were more stable than GPH2-loaded MPs. Wang et al. [22] reported that positively charged MPs could easily adhere to the epithelial cells through electrostatic interactions with the negatively charged mucin glycosyl, which allows the prolongation of their retention time to the absorption site, and improved thereby their oral bioavailability. Indeed, Du et al. [12] stated that the addition of peptide fractions in the chitosan solution may have huge influence on the zeta potential of the nanoparticles.

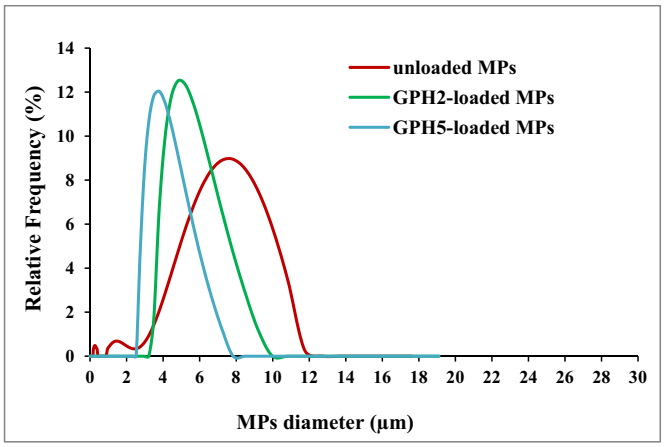

Fig. 1. Particles size distribution of unloaded and GPH-loaded microparticles.

The particle size is an important parameter that affects the properties and the biodistribution of MPs. Particle size distribution curves, illustrated in Fig. 1, show a monomodal distribution with one peak representing a predominant size. It can also be shown in Table 1 that the mean particles size significantly decreased from 7.26 μm for unloaded MPs to 4.81 and 3.77 μm for GPH2- and GPH5-loaded MPs, respectively. The obtained results could be explained by the fact that the addition of peptides into CH solution enhances the formation of electrostatic interactions between their charged groups, and also, as a result, the decrease of MPs volume and diameter. In contrast, Anandhakumar et al. [21] stated that chitosan nanoparticles size increase with the collagen peptides content increases. Du et al. [12] found that the mean particle size increased with the increase of peptides content.

Table 1
Zeta potential, mean particle size, encapsulation efficiency (EE) and loading capacity (LC) of MPs.

MPs	GPH concentration (mg/ml)	Z-potential (mV)	Mean particles size (μm)	EE (%)*	LC (%)**
Unloaded MPs	0	51.43 ± 0.7^a	7.26 ± 0.01^a	–	–
GPH2-loaded MPs	2	35.43 ± 1.6^b	4.81 ± 0.06^b	44 ± 0.2^a	38.6 ± 0.2^a
GPH5-loaded MPs	5	50.00 ± 2.3^a	3.78 ± 0.01^c	57.8 ± 1.0^b	82.6 ± 1.5^b

Data are presented as mean ± SD (n = 3). Different letters within a column indicate significant differences among GPH concentrations ($p < 0.05$). MPs: microparticles. CH: Blue crab chitosan; GPH: goby protein hydrolysate prepared using triggerfish digestive proteases.
* g per 100 g of GPH concentration.
** g per 100 g of MPs.

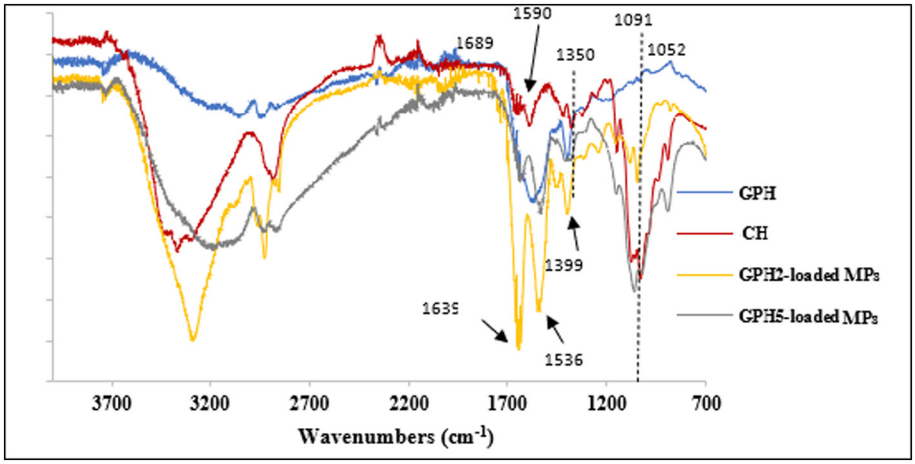

Fig. 2. FTIR spectra of GPH, CH and microparticles.

3.1.2. FT-IR analysis

The freeze-dried GPH, CH and microcapsules were also characterized using FT-IR spectroscopy. Characteristic bands of chitosan at 3402 cm^{-1}, 2935–2884 cm^{-1}, 1689 cm^{-1}, 1586 cm^{-1} and 1432 cm^{-1} assigned to O—H stretching bands, C—H stretching bands, amide I (C=O), amide II (-NH_2 vibrations) and -CH_2 binding [23], respectively, were presented in the infrared profile of CH powder (Fig. 2). In addition, specific absorption peaks of chitosan assigned to asymmetrical deformation of CH_3 groups at 1351 cm^{-1}, anti-symmetric stretching of C-O-C and C—H stretching at 1101 cm^{-1} and pyranoside ring stretching vibration at 596 cm^{-1} were detected.

For FT-IR peptides spectrum, characteristic peaks of proteins at 3167 cm^{-1} (N—H stretching), 2926 cm^{-1} (C—C asymmetric stretch), 1548 cm^{-1} (amide II, C—N and N—H stretching) and 1385 cm^{-1} (C—H bending) were observed in Fig. 2. Regarding GPH-charged MPs profiles, the wavenumber at 3402 cm^{-1} in CH curve, ascribed to the amide A band, was shifted to 3293 cm^{-1} and 3165 cm^{-1} for GPH2- and GPH5-loaded CH MPs, respectively. Besides, it became broader in MPs containing 5 mg/ml of peptides, suggesting the strong hydrogen interactions involved in the formation of the MPs subsequent to ionic gelation. The same trends were stated by Hosseini et al. [6], Leonida et al. [24] and Rampino et al. [25]. Compared to the free GPH spectrum, a double stretching at 1639 and 1536 cm^{-1} was evident in the spectra of loaded MPs; this may be assigned to the formation of α-helix conformation [26]. Furthermore, a decrease in the frequency of amide II of loaded MPs to 1536 cm^{-1} was noted, indicating therefore the formation of electrostatic interactions between biopeptides, chitosan and TPP through their charged groups [5,23,27].

3.1.3. Microstructure investigation

Fig. 3 presents the morphology of the MPs obtained by SEM. MPs had a spherical form with an average diameter (<1 μm) smaller than that measured by Zetasizer. This finding could be due to the aggregation of the MPs during the drying step. It should be pointed out that the particle size obtained by the DLS method is a hydrodynamic diameter. Similar observations were described by Hosseini et al. [6], Du et al. [12] and Piras et al. [28]. Nevertheless, the initial concentration of peptides did not affect the morphology of chitosan-based MPs.

3.1.4. Thermogravimetric analysis

The thermogravimetric analysis is widely applied to assess the thermal stability of microcapsules, in which the mass loss was measured as a function of temperature. The TGA thermograms, plotted in Fig. 4a, show that the weight loss of the samples decreased with the increase of temperature. The residual weights of CH and peptides after incubation at 700 °C were 26% and 25%, respectively. It is interesting to note that the interaction and crosslinking of chitosan with TPP increased the stability of CH against temperature (residual weight of 47.55% at 700 °C). The encapsulated peptides show higher thermal stability than that of free peptides with residual weights of 48.36% and 40.62% for GPH2- and GPH5-loaded MPs, respectively. The degradation temperatures (Td), which correspond to the highest amount of weight loss, are

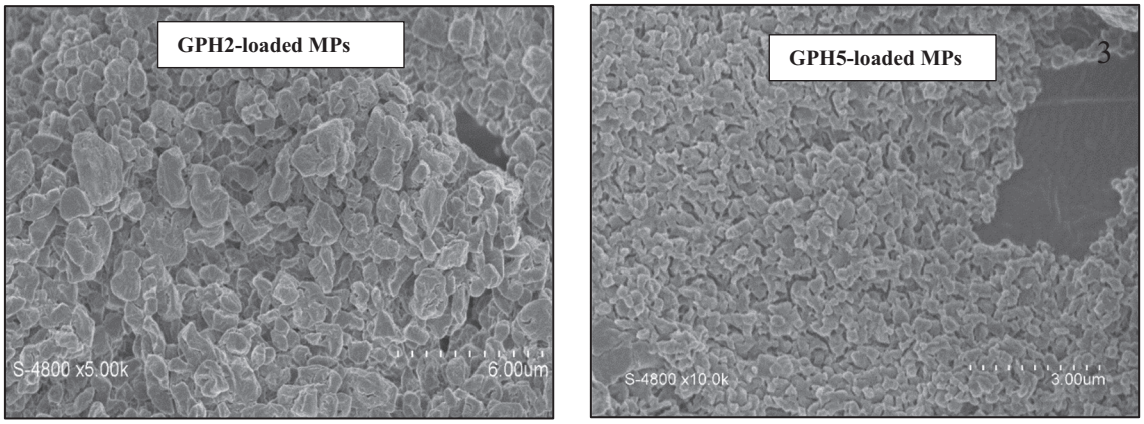

Fig. 3. SEM images of GPH-loaded microparticles.

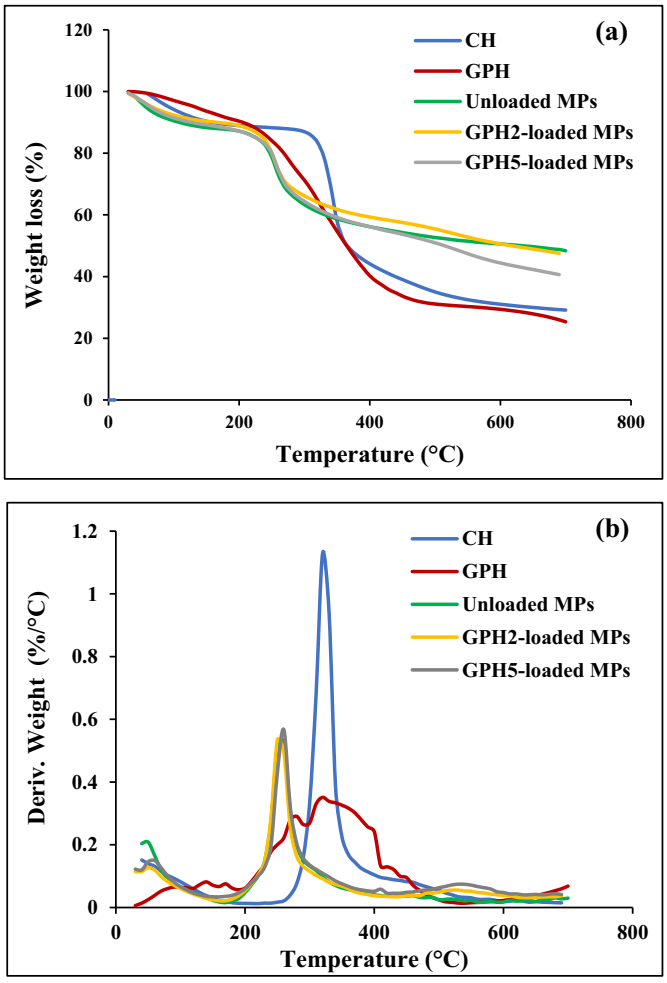

Fig. 4. ATG (a) and DTG (b) profiles of GPH, CH and microparticles.

depicted through DTG thermograms (Fig. 4b). The spectrum of GPH shows two major degradation phases. The first weight loss was detected at 100 °C, linked to the water evaporation and the second slope of weight loss was detected at temperatures ranging from 220 to 420 °C, attributed to the decomposition of peptides. On the other hand, CH degradation curve reveals that the main dehydration and degradation of chitosan rings was detected at 320 °C.

The DTG curve of unloaded MPs shows a single weight loss peak at 260 °C, which could be assigned to the decomposition of the CH/TPP (Fig. 4b). Similarly, GPH-charged MPs curves reveal the vanishing of chitosan and peptides degradation peaks and the emergence of the only degradation peak at 260 °C. This proves, once again, the entrapment efficiency of GPH peptides into the chitosan-TPP capsules and their protection against decomposition at high temperatures.

3.2. Encapsulation efficiency and loading capacity of MPs

The EE and LC of MPs are shown in Table 1. GPH5-loaded MPs had higher EE (57.83%) than GPH2-loaded MPs (43.95%), indicating that the EE increases with the increase of initial peptides concentration added to CH solution. The improvement of EE as a function of peptides concentration could be explained by the increase of hydrogen interactions between the peptides and TPP. Reports focused on the evaluation of the effect of peptides content on their EE are inconclusive. According to Keawchaoon & Yoksan [29], the EE of carvacrol into CH/TPP systems increased with increasing bioactive molecules content. Gan & Wang [30] reported the increase of the EE of albumin in CH/TPP microparticles from 38.7 to 72.5% when the initial concentration of protein increased from 0.25 to 1.50 mg/ml. In contrast, Piras et al. [28] demonstrated that low concentration of peptides led to a high encapsulation degree.

Additionally, we may notice the increase of the LC of MPs, when increasing the amount of peptides ($p < 0.05$), as mentioned in Table 1. In fact, the LC values increased from 38.68% for GPH2-loaded MPs to 82.62% for GPH5-loaded MPs. Similar results have also reported the increase of LC as a function of protein or peptides content [29,30]. According to Dunn et al. [31], the content of loaded molecules in nanoparticles is highly dependent on the non-covalent and covalent interactions established between biomolecules and the surface functional group. Moreover, the increase in the amount of peptide encapsulated in the GPH5-loaded MPs may be related to their zeta potential which is higher than that of GPH2-loaded MPs.

3.3. Release profiles of peptides from MPs

The encapsulated biopeptides can be released from the colloidal particles through a variety of mechanisms, including changes in molecular interactions and increased pore size of particles, as well as diffusion and

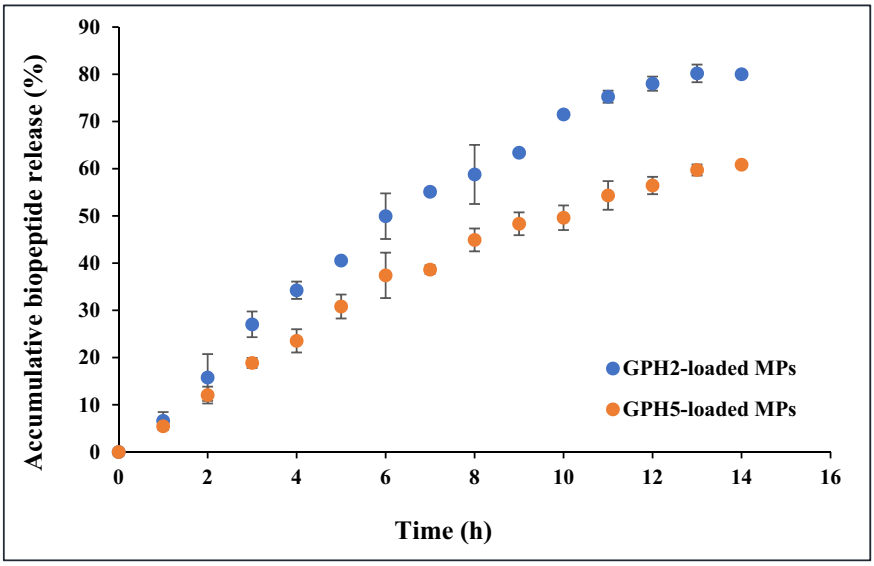

Fig. 5. *In vitro* release profiles of biopeptide from GPH2- and GPH5-loaded MPs (37 °C; PBS buffer). Release percentages are expressed as the mean ± SD (n = 3).

Table 2
Kinetic parameters obtained through fitting to several mathematical kinetic models of peptides release profiles.

Microparticles	Kinetic models								
	Zero order		First order		Higuchi model		Korsmeyer-Peppas model		
	R^2	k	R^2	k	R^2	k	R^2	k	n
GPH2-loaded MPs	0.973	0.024	0.9928	0.0009	0.981	0.620	0.996	0.106	0.783
GPH5-loaded MPs	0.9736	0.032	0.995	0.0005	0.981	0.825	0.995	0.151	0.772

erosion [14]. The *in vitro* biopeptides release profiles from CH-based MPs in PBS buffer can be described as a biphasic process (Fig. 5). Indeed, the release profiles showed a fast-initial release stage within the first 12 h, possibly attributed to the diffusion of peptides loaded to MP's external layer. At the second stage, a slow biopeptides release was occurred till 14 h, which can be accredited to the diffusion of peptides after the swelling and/or degradation of the wall matrix of chitosan/TPP MPs [14]. A similar release profile was reported by Hosseini et al. [6] for the release of common kilka antioxidant peptides.

In terms of percentage, GPH5-loaded MPs released 60.84% of the encapsulated biopeptides, while accumulative biopeptides release of more than 80% was obtained with GPH2-loaded MPs after 14 h of incubation (Fig. 5). Hosseini et al. [6] also reported that the percentage of released peptides decreased when their initial concentration increased from 1 to 5 mg/ml. The particle size of MPs influences the peptides delivery rate.

3.4. Determination of release mechanisms

Mathematical modeling of release process is primordial to get a better idea of the delivery phenomenon. The release kinetics of peptides from chitosan MPs was evaluated by fitting the biopeptides release data to four mathematical models (*e.g.* zero order, first order, Higuchi and Korsmeyer-Peppas models). The analysis of correlation coefficients (r^2) of linear relationship between biopeptides liberation and time was established for the sake of the evaluation of the release mechanism.

The best kinetic model of MPs was evaluated through the determination of the highest r^2 value, as shown in Table 2. Overall, the release kinetics of biopeptides from chitosan MPs fitted well with the first-order (0.992–0.995) and Korsmeyer–Peppas (0.995–0.996) models.

The release mechanism of biopeptides from chitosan MPs was carried out using the Korsmeyer–Peppas model, in which the release exponent "n" was related to the release mechanism and it illustrated the type of drug transport. Regarding spherical system, $n < 0.43$ is assigned to Fickian diffusion of drug from microcapsules. A release exponent ranging from 0.43 to 0.85 indicates an anomalous transport, and the drug release, in this case, is monitored by diffusion- and swelling processes. The value $n > 0.85$ is considered as case II transport, which is involved in polymer relaxation during swelling diffusion and matrix erosion [32].

As seen in Table 2, peptides release data is fitted to the Korsmeyer-Peppas model, with n values around 0.77 and 0.78 for peptides released from GPH2- and GPH5-loaded MPs, respectively. The obtained values reveal that the release mechanism of GPH peptides from the blue crab chitosan system follows non-Fickian diffusion (anomalous transport), indicating that the peptides release rate depends simultaneously on the swelling and on the diffusion processes.

The mechanism of peptides release from chitosan MPs in water could be divided into two stages: i) the first stage consists in the passive diffusion of peptides located near the surface of the microcapsules; ii) during the second part, the chitosan MPs absorb water and swell, leading to the amplification of diffusion spaces and to the release of the peptides located in the MPs.

3.5. Antioxidant activity of loaded MPs

The DPPH method measures hydrogen atom donating ability of biopeptides. The DPPH radical-scavenging activity of unloaded and loaded MPs was investigated and presented in Fig. 6. It is worthy to note a positive correlation between the biopeptides concentrations and the radical-scavenging potential of loaded MPs. In fact, GPH5-loaded MPs manifested high antioxidant activity (54%) compared to GPH2-loaded MPs (44%); while unloaded MPs displayed only 28% of antioxidant activity. These findings clearly indicate that loaded-biopeptides significantly improved the antioxidant capacity of the MPs ($p < 0.05$).

The evaluation of the metal chelating activity of unloaded and loaded microparticles was also carried out. As shown in Fig. 6, all loaded

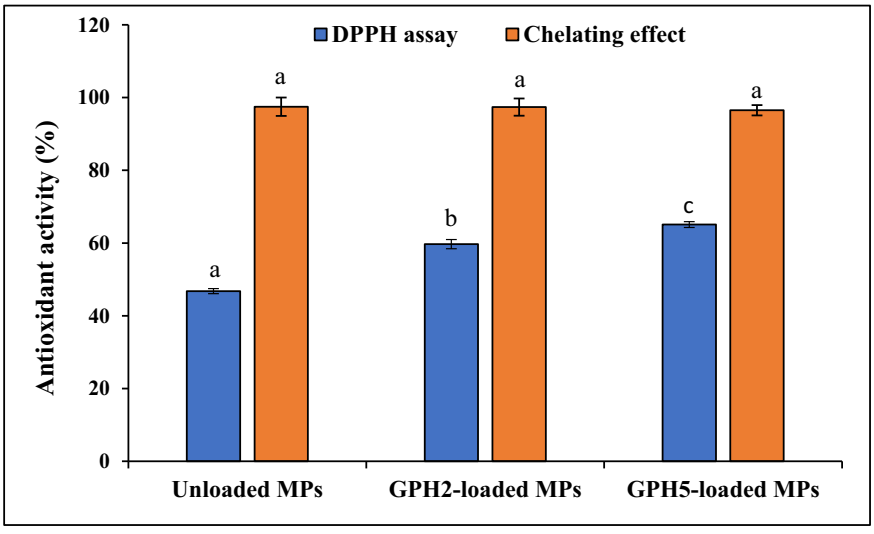

Fig. 6. DPPH scavenging activity (a) and chelating power (b) of unloaded and loaded microparticles. Data are presented as the mean ± SD (n = 3). [a–c] Different capital letters indicate significant differences in the release of peptides at the same time among the MPs ($p < 0.05$).

MPs exhibited an interesting chelating effect, which was similar to unloaded MPs. The obtained results indicated the potential of chitosan MPs to catch iron ion.

4. Conclusion

A chitosan-based MPs encapsulating antioxidant biopeptides were successfully produced *via* ionic gelation method. FT-IR spectra reported an effective ionic cross-linking between CH and peptides as a function of peptide concentrations, which could be considered as driving force for GPH-loaded MPs elaboration. The particles had spherical form as confirmed by SEM. By increasing the concentration of biopeptides into chitosan solution, EE is increased. The *in vitro* release analysis showed that the concentration of biopeptides in the MPs influenced its release rate. The release mechanism of GPH peptides from the chitosan system follows non-Fickian diffusion, indicating that the biopeptides release rate depends simultaneously on the swelling and diffusion processes. Hence, GPH-loaded MPs exhibited a potent antioxidant activity compared to unloaded MPs.

CRediT authorship contribution statement

Rim Nasri: Conceptualization, Methodology, Investigation, Visualization, Writing - original draft, Writing - review & editing. **Marwa Hamdi:** Investigation. **Sana Souid:** Investigation. **Suming Li:** Visualization. **Maha Karra-Châabouni:** Visualization. **Moncef Nasri:** review & editing.

Declaration of competing interest

The authors declare no competing interests.

Acknowledgements

Financial assistance for this study was provided by the Ministry of Higher Education and Scientific Research, Tunisia (grant no. 18PJEC08-01). This research work was conducted in the framework of PHC-Utique Program (partenariat Hubert Curien « Utique » du Ministère de l'Europe et des Affaires Etrangères français et du Ministère de l'Enseignement et de la Recherche Scientifique tunisien) financed by CMCU (Comité mixte de coopération universitaire), grant no.: 19G0815.

References

[1] M. Nasri, Protein hydrolysates and biopeptides: production, biological activities, and applications in foods and health benefits. A review, Adv. Food Nutr. Res. 81 (2017) 109–159.
[2] O. Abdelhedi, R. Nasri, L. Mora, M. Jridi, F. Toldrá, M. Nasri, *In silico* analysis and molecular docking study of angiotensin I-converting enzyme inhibitory peptides from smooth-hound viscera protein hydrolysates fractionated by ultrafiltration, Food Chem. 15 (2018) 453–463.
[3] W. Yu, C.J. Field, J. Wu, Purification and identification of anti-inflammatory peptides from spent hen muscle proteins hydrolysate, Food Chem. 253 (2018) 101–107.
[4] R. Nasri, I. Ben Amor, A. Bougatef, N. Nedjar-Arroume, P. Dhulster, J. Gargouri, M. Karra Châabouni, M. Nasri, Anticoagulant activities of goby muscle protein hydrolysates, Food Chem. 133 (2012) 835–841.
[5] R. Nasri, I. Younes, M. Jridi, M. Trigui, A. Bougatef, N. Nedjar-Arroume, P. Dhulster, M. Nasri, M. Karra-Châabouni, ACE inhibitory and antioxidative activities of Goby (*Zosterissessor ophiocephalus*) fish protein hydrolysates: effect on meat lipid oxidation, Food Res. Int. 54 (2013) 552–561.
[6] S.F. Hosseini, M.R. Soleimani, M. Nikkhah, Chitosan/sodium tripolyphosphate nanoparticles as efficient vehicles for antioxidant peptidic fraction from common kilka, Int. J. Biol. Macromol. 111 (2018) 730–737.
[7] P.X. Gong, B.K. Wang, Y.C. Wu, Q.Y. Lia, B.W. Qin, H.J. Li, Release of antidiabetic peptides from *Stichopus japonicas* by simulated gastrointestinal digestion, Food Chem. 315 (2020) 126273.
[8] R. Nasri, O. Abdelhedi, I. Jemil, I. Daoued, K. Hamden, C. Kallel, A.F. Elfeki, M. Lamri-Senhadji, A. Boualgua, A. Nasri, M. Karra-Châabouni, Ameliorating effects of goby fish protein hydrolysates on high-fat-high-fructose diet-induced hyperglycemia, oxidative stress and deterioration of kidney function in rats, Chem. Biol. Interact. 2425 (2015) 71–80.
[9] A. Mohan, S.R.C.K. Rajendran, Q.S. He, L. Bazinet, C.C. Udenigwe, Encapsulation of food protein hydrolysates and peptides: a review, RSC Adv. 5 (2015) 79270–79278.
[10] N. Rezaei, F. Mehrnejad, Z. Vaezi, M. Sedghi, S.M. Asghari, H. Naderi-Manesh, Encapsulation of an endostatin peptide in liposomes: stability, release, and cytotoxicity study, Colloids Surf. B Biointerfaces 185 (2020) 110552.
[11] M.K. Danish, G. Vozza, H.J. Byrne, J.M. Frias, S.M. Ryan, Comparative study of the structural and physicochemical properties of two food derived antihypertensive tri-peptides, Isoleucine-Proline-Proline and Leucine-Lysine-Proline encapsulated into a chitosan-based nanoparticle system, Innov. Food Sci. Emerg. Technol. 44 (2017) 139–148.
[12] Z. Du, J. Liu, T. Zhang, Y. Yu, Y. Zhang, J. Zhai, H. Huang, S. Wei, L. Ding, B. Liu, A study on the preparation of chitosan-tripolyphosphate nanoparticles and its entrapment mechanism for egg white derived peptides, Food Chem. 286 (2019) 530–536.
[13] B. Zhang, X. Zhang, Separation and nanoencapsulation of antitumor polypeptide from *Spirulina platensis*, Biotechnol. Prog. 29 (2013) 1230–1238.
[14] D.J. McClements, Encapsulation, protection, and delivery of bioactive proteins and peptides using nanoparticle and microparticle systems: a review, Adv. Colloid Interf. Sci. 253 (2018) 1–22.
[15] H. Hamdi, S. Hajji, S. Affes, W. Taktak, H. Mâalej, M. Nasri, R. Nasri, Development of a controlled bioconversion process for the recovery of chitosan from blue crab (*Portunus segnis*) exoskeleton, Food Hydrocoll. 77 (2018) 534–548.
[16] O.H. Lowry, N.J. Rosebrough, L.A. Farr, R.J. Randall, Protein measurement with the Folin phenol reagent, J. Biol. Chem. 193 (1951) 265–275.
[17] P. Bersuder, M. Hole, G. Smith, Antioxidants from a heated histidine–glucose model system. I: investigation of the antioxidant role of histidine and isolation of antioxidants by high-performance liquid chromatography, J. Am. Oil Chem. Soc. 75 (1998) 181–187.
[18] E.A. Decker, B. Welch, Role of ferritin as a lipid oxidation catalyst in muscle food, J. Agric. Food Chem. 38 (1990) 674–677.
[19] X.Z. Shu, K.J. Zhu, Controlled drug release properties of ionically cross-linked chitosan beads: the influence of anion structure, Int. J. Pharm. 233 (2002) 217–225.
[20] M.K. Sureshkumar, D. Das, M.B. Mallia, Adsorption of uranium from aqueous solution using chitosan-tripolyphosphate (CTPP) beads, J. Hazard. Mater. 184 (2010) 65–72.
[21] S. Anandhakumar, G. Krishnamoorthy, K.M. Ramkumar, A.M. Raichur, Preparation of collagen peptide functionalized chitosan nanoparticles by ionic gelation method: an effective carrier system for encapsulation and release of doxorubicin for cancer drug delivery, Mater. Sci. Eng. C 70 (2017) 378–385.
[22] F. Wang, Y. Yang, X. Ju, C.C. Udenigwe, R. He, Polyelectrolyte complex nanoparticles from chitosan and acylated rapeseed cruciferin protein for curcumin delivery, J. Agric. Food Chem. 66 (2018) 2685–2693.
[23] C.P. Kiilll, H.D.S. Barud, S.H. Santagneli, S.J.L. Ribeiro, A.M. Silva, A. Tercjak, J. Gutierrez, A.M. Pironi, M.P.D. Gremião, Synthesis and factorial design applied to a novel chitosan/sodium polyphosphate nanoparticle via ionotropic gelation as an RGD delivery system, Carbohyd. Polym. 157 (2017) 1695–1702.
[24] M.D. Leonida, S. Banjade, T. Vo, G. Anderle, G.J. Haas, N. Philips, Nanocomposite materials with antimicrobial activity based on chitosan, Int. J. Nano Biomater. 3 (2011) 316–334.
[25] A. Rampino, M. Borgogna, P. Blasi, B. Bellich, A. Cesàro, Chitosan nanoparticles: preparation, size evolution and stability, Int. J. Pharm. 455 (2013) 219–228.
[26] E.S. Bonwell, D.L. Wetzel, Innovative FT-IR imaging of protein film secondary structure before and after heat treatment, J. Agric. Food Chem. 57 (2009) 10067–10072.
[27] P. Chanphai, H.A. Tajmir-Riahi, Chitosan nanoparticles conjugate with trypsin and trypsin inhibitor, Carbohyd. Polym. 144 (2016) 346–352.
[28] A.M. Piras, G. Maisetta, S. Sandreschi, M. Gazzarri, C. Bartoli, L. Grassi, S. Esin, F. Chiellini, G. Batoni, Chitosan nanoparticles loaded with the antimicrobial peptide temporin B exert a long-term antibacterial activity in vitro against clinical isolates of Staphylococcus epidermidis, Front. Microbiol. 6 (2015) 372.
[29] L. Keawchaoon, R. Yoksan, Preparation, characterization and in vitro release study of carvacrol-loaded chitosan nanoparticles, Colloids Surf. B: Biointerfaces 84 (2011) 163–171.
[30] Q. Gan, T. Wang, Chitosan nanoparticle as protein delivery carrier-systematic examination of fabrication conditions for efficient loading and release, Colloids Surf. B: Biointerfaces 59 (2007) 24–34.
[31] A.E. Dunn, D.J. Dunn, M. Lim, C. Boyer, N.T.K. Thanh, Recent developments in the design of nanomaterials for photothermal and magnetic hyperthermia induced controllable drug delivery, Nano 2 (2013) 225–254.
[32] P.L. Ritger, N.A. Peppas, A simple equation for description of solute release II. Fickian and anomalous release from swellable devices, J. Control. Release 5 (1987) 37–42.